Self-Assembly of Formic Acid/ Polystyrene-*block*-poly(4-vinylpyridine) Complexes into Vesicles in a Low-Polar Organic Solvent Chloroform

Huisheng Peng, Daoyong Chen,* and Ming Jiang

Department of Macromolecular Science and The Key Laboratory of Molecular Engineering of Polymers, Fudan University, Shanghai 200433, China

Received May 21, 2003. In Final Form: September 29, 2003

Self-assembly of block copolymers in solutions and the resultant polymeric nano-objects have attracted considerable interest in both theoretical and applied research fields.[1−7] Recently, a number of studies on the self-assembly of complexes of block copolymers/low-molecular mass compounds (LMC, including surfactants and other molecules with a polar head and a nonpolar tail) were reported. Since the relative amount of LMC and the binding are adjustable, Ikkala et al. used the complexes to prepare materials with different morphologies and on−off properties in bulk.[8−11] *In aqueous media*, the self-assembly of the complex of LMC and a block copolymer may result in vesicles alone,[12,13] micellar clusters, or precipitation,[14] depending on the dispersion state of the block copolymer in water before mixed with LMC. However, *in low-polar organic solvents* in which the nonpolar tails of LMC are soluble, the self-assembly leads to different results.[15,16] The block copolymers capable of forming complexes with LMC contain at least one block with a certain number of polar groups, so the binding with LMC usually increases their solubility in low-polar organic solvents.[16] Therefore, no regular aggregates resulting from the self-assembly of the complexes of LMC and block copolymers *in organic solvents* have been reported. This brought up a question to us, i.e., what would the complexes behave like in the low-polar organic solvents if we reduce the length of the lipophilic tails of LMC or even remove them? We studied the complexation of polystyrene-*b*-poly(4-vinylpyridine) (PS-*b*-P4VP) with linear aliphatic acids in chloroform. The results show that the resultant complexes may self-assemble to form nano-sized aggregates (vesicles) or exist in a molecularly dispersed state, depending on the length of the aliphatic chains.

Table 1. Laser Light Scattering Characterization of the Aggregates in $CHCl_3$ at 25 °C

	MR = 1/5	MR = 1/3	MR = 1/2	MR = 1/1
$M_{w,particle}$[a]	6.02×10^5	4.06×10^6	5.71×10^6	1.49×10^7
$\langle R_g \rangle$/nm	68	51	55	69
$\langle R_h \rangle$/nm	53	55	62	84
$\langle R_g \rangle / \langle R_h \rangle$	1.28	0.93	0.89	0.82
$N_{aggregation}$[b]	9	65	92	241
$\langle \rho \rangle$/(g/cm^3)[c]	0.00016	0.0094	0.0095	0.01
$\mu_2/\langle \Gamma \rangle^2$ [d]	0.04	0.1	0.1	0.1

[a] Average weight of each aggregate. [b] Average number of the complex inside each aggregate. [c] The average density of the aggregates, calculated based on $M_{w,particle}$ and $\langle R_h \rangle$.[19] [d] The polydispersity index of the size distribution.[20]

Chloroform is a common solvent for the block copolymer PS-*b*-P4VP, as well as a solvent for *stearic acid* (SA), *decanoate* (DA), *acetic acid* (AA), and *formic acid* (FA). When PS-*b*-P4VP (the weight average molecular weights of the PS and P4VP blocks are 33 000 and 29 000 respectively; the M_w/M_n of the block copolymer is 1.37) was mixed with SA, DA, and AA in chloroform, the mixture solutions remained transparent. However, ^{13}C NMR spectra of the mixtures in deuterated chloroform show that the peak associated with the carbon atoms in the carboxyl of the acids shifts from 178.0 to 175.5 ppm. In addition, in the spectra of the stoichiometric mixtures, no signals of the acids in the unbound state were detected. These results indicate that the copolymer can form soluble complexes with the aliphatic acids SA, DA, and AA and that in the stoichiometric mixtures almost all the carboxyl groups of the acids bind with the pyridine groups. In other words, the complexation is irreversible. This agrees with the results obtained by Ikkala et al. on the complexation between P4VP and 3-pentadecylphenol.[9,17,18]

When the solutions of the complexes of PS-*b*-P4VP with SA, DA, and AA in chloroform were characterized by dynamic light scattering (DLS), no aggregates were detected. While the block copolymer was mixed with the smallest acid FA under the identical conditions, blue opalescence appeared simultaneously. The solution at the concentration of the block copolymer of 1.0 mg/mL was mixed with FA at different molar ratios of FA to the pyridine rings in the block copolymer (MR), and then the mixtures were studied by static light scattering (SLS) and DLS. The results are presented in Table 1.

It is shown in Table 1 that aggregation took place in the mixtures of PS-*b*-P4VP with FA in chloroform when MR ≥ 1/5, resulting in aggregates with the average hydrodynamic radiuses ($\langle R_h \rangle$) from 53 to 84 nm. The aggregates have a narrow size distribution with a regular spherical morphology, indicated by the relatively low polydispersity indexes ($\mu^2/\langle \Gamma \rangle^2 \approx 0.1$) and almost no dependence of the sizes on the measurement angles.

The values of $\langle R_g \rangle / \langle R_h \rangle$ ($\langle R_g \rangle$ is the average radius of gyration measured by SLS) and the density of the aggregates are also presented in Table 1, which can be

(1) Webber, S. E. *J. Phys. Chem. B* **1998**, *102*, 2618.
(2) Moffitt, M.; Khougaz, K.; Eisenberg, A. *Acc. Chem. Res.* **1996**, *29*, 95.
(3) Jenekhe, S. A.; Chen, X. L. *Science* **1999**, *283*, 372.
(4) Kataoka, K.; Harada, A.; Nagasaki, Y. *Adv. Drug Delivery Rev.* **2001**, *47*, 113.
(5) Moffitt. M.; Vali, H.; Eisenberg, A. *Chem. Mater.* **1998**, *10*, 1021.
(6) Klingelhofer, S.; Heitz, W.; Greiner, A.; Oestreich, S.; Forster, S.; Antonietti, M. *J. Am. Chem. Soc.* **1997**, *119*, 10116.
(7) Discher, B. M.; Won, Y. Y.; Ege, D. S.; Lee, J. C. M.; Bates, F. S.; Discher, D. E.; Hammer, D. A. *Science* **1999**, *284*, 1143.
(8) Ruokolainen, J.; Mäkinen, R.; Torkkeli, M.; Mäkelä, T.; Serimaa, R.; ten Brinke, G.; Ikkala, O. *Science* **1998**, *280*, 557.
(9) Ruokolainen, J.; ten Brinke, G.; Ikkala, O. *Adv. Mater.* **1999**, *11*, 777.
(10) Ruokolainen, J.; Torkkeli, M.; Serimaa, R.; Komanschek, E.; ten Brinke, G.; Ikkala, O. *Macromolecules* **1997**, *30*, 2002.
(11) de Moel, K.; Alberda van Ekenstein, G. O. R.; Nijland, H.; Polushkin, E.; ten Brinke, G.; Mäki-Ontto, R.; Ikkala, O. *Chem. Mater.* **2001**, *13*, 4580.
(12) Kabanov, A. V.; Bronich, T. K.; Kabanov, V. A.; Yu, K.; Eisenberg, A. *J. Am. Chem. Soc.* **1998**, *120*, 9941.
(13) Bronich, T. K.; Ouyang, M.; Kabanov, V. A.; Eisenberg, A.; Szoka, F. C., Jr.; Kabanov, A. V. *J. Am. Chem. Soc.* **2002**, *124*, 11872.
(14) Lysenko, E. A.; Bronich, T. K.; Slonkina, E. V.; Eisenberg, A.; Kabanov, V. A.; Kabanov, A. V. *Macromolecules* **2002**, *35*, 6351.
(15) Bakeev, K. N.; Lysenko, E. A.; MacKnight, W. J.; Zezin, A. B.; Kabanov, V. A. *Colloids Surfaces, A* **1999**, *147*, 263.
(16) Lysenko, E. A.;Bronich, T. K.; Slonkina, E. V.; Eisenberg, A.; Kabanov, V. A.; Kabanov, A. V. *Macromolecules* **2002**, *35*, 6344.
(17) Ruokolainen, J.; ten Brinke, G.; Ikkala, O. *Macromolecules* **1996**, *29*, 3409.
(18) Ruokolainen, J.; Saariaho, M.; Ikkala, O.; ten Brinke, G.; Thomas, E. L.; Torkkeli, M.; Serimaa, R. *Macromolecules* **1999**, *32*, 1152.

10.1021/la0348721 CCC: $25.00
Published on Web 11/22/2003

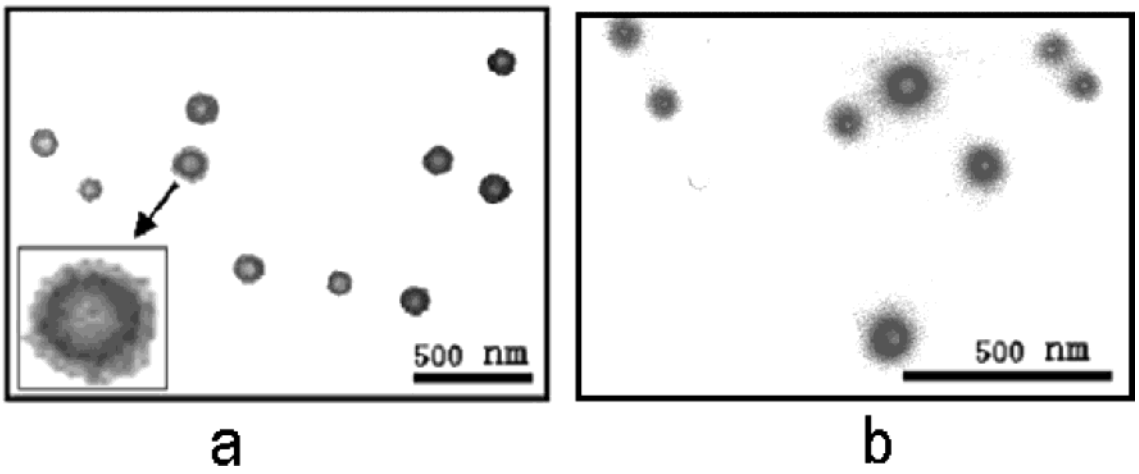

Figure 1. TEM graphs of the vesicles resulting from the complexation between FA and PS-b-P4VP in $CHCl_3$: (a) MR = 1/3; (b) MR = 1/1.

used to characterize their morphology.[19,21,22] Theoretically, for a uniform nondraining solid sphere, a nondraining thin shell vesicle, a hyperbranched cluster, and a random coil, the ratios of $\langle R_g\rangle/\langle R_h\rangle$ are about 0.774, 1.0, 1.0−1.3 and 1.5−1.8, respectively.[19,22] While experimentally, for a polymeric micelle, $\langle R_g\rangle/\langle R_h\rangle$ is often less than 0.774 since the density of the core is remarkably larger than that of the shell,[23,24] for a polymeric vesicle, $\langle R_g\rangle/\langle R_h\rangle$ is usually less than 1.0, depending on the thickness of the wall.[19] In this work, at MR between 1 and 1/3, the values of $\langle R_g\rangle/\langle R_h\rangle$ range from 0.82 to 0.93, being obviously larger than 0.774 and in the range for polymeric hollow spheres; [19] the densities are around 0.0095 g/cm^3, being much less than that of micelles.[24] Therefore, it is reasonable to think that the aggregates are in the form of vesicles. This is further proved by transmission electron microscopy (TEM) observations. The TEM graph at MR of 1/3 (Figure 1a) shows a typical morphology of vesicles. From the image at a larger magnification (Figure 1a, inset), one can see the three-layer structure of the vesicle with a dark high-density middle layer sandwiched between the outer and inner layers. Furthermore, with the increase of MR, the value of $\langle R_g\rangle/\langle R_h\rangle$ decreases (Table 1) remarkably, indicating the increase in the ratio of the wall thickness to the radius of the resultant vesicles.[25] This is consistent with the TEM observations (Figure 1b). Due to the large wall thickness, the morphology of the particles in Figure 1b is the intermediate between the morphology of solid spheres and that of typical vesicles.

Nevertheless, it seems that the sizes and the change of the sizes with MR based on the TEM observations are different from those obtained by DLS measurements. For simplicity of description, we use $D_B{}^A$ to denote the diameter measured by A (A represents TEM or DLS) at MR of B (B is 1/3 or 1/1). $D_{1/3}{}^{TEM}$ (Figure 1a) is from ca. 115 to 155 nm and $D_{1/1}{}^{TEM}$ (Figure 1b) ca. 90 to 151 nm, while $D_{1/3}{}^{DLS}$ and $D_{1/3}{}^{DLS}$ are 101 and 168 nm, respectively (Table 1). Two points should be noted: (1) $D_{1/3}{}^{TEM}$ is larger than $D_{1/3}{}^{DLS}$ whereas $D_{1/1}{}^{TEM}$ is less than $D_{1/1}{}^{DLS}$; (2) $D_{1/1}{}^{DLS}$ is larger than $D_{1/3}{}^{DLS}$ whereas $D_{1/1}{}^{TEM}$ is smaller than $D_{1/3}{}^{TEM}$. Similar phenomena were reported by Eisenberg et al.[26] In fact or in principle, several factors may make contributions to the difference between D^{DLS} and D^{TEM} of the same aggregates. (1) D^{DLS} of the aggregates is that of the equivalent nondraining spheres whereas D^{TEM} is based on the outline of the aggregates. This makes D^{DLS} smaller than D^{TEM} due to the drainable nature of the shell. (2) The spreading out of aggregates on the Formvar grid onto which they are deposited may result in D^{DLS} smaller than D^{TEM} as well.[27] (3) The shrinking upon drying and in some cases the invisibility of the shell-forming component by TEM may cause D^{DLS} larger than D^{TEM}.[26,28] It is obvious that the extent of the contribution made by each of the factors is related to the morphology and composition of the aggregates. In the present work, the composition and the morphology of the aggregates at MR of 1/3 are different from those at MR of 1/1. Therefore, it is possible that in the case of MR being 1/3 the contributions made by the factors 1 and 2 are dominant, while at MR of 1/1 the contribution by the factor 3 is the most important.

When *MR* decreases to 1/5, the average number of the block copolymer chains inside each aggregate ($N_{aggregation}$) declines to 9; the average density (ρ) of the aggregates is as low as 1.6×10^{-4} g/cm^3. This density is about 3 orders of magnitude smaller than that of polymeric micelles[21] and one-tenth of that of polymeric hollow spheres.[19] Meanwhile, the $\langle R_g\rangle/\langle R_h\rangle$ increases to 1.28, in the range for a hyperbranched cluster. Therefore, the aggregates formed with a small proportion of FA are no longer a typical vesicular form. This implies that there is a minimum MR, which should be greater than 1/5 for the complex to build relatively dense aggregates such as vesicles. As is mentioned above, the density of aggregates at MR of 1/5 is very low. This maybe due to the fact that only 1/5 of pyridine units in the block copolymer are connected with FA and aggregated, so the structure of the aggregates

(19) Duan, H. W.; Chen, D. Y.; Jiang, M.; Gan, W. J.; Li, S. J.; Wang, M.; Gong, J. *J. Am. Chem. Soc.* **2001**, *123*, 12097.
(20) Chu, B.; Wang, Z.; Yu, J. *Macromolecules* **1991**, *24*, 6832.
(21) Zhang, G. Z.; Niu A. Z.; Peng S. F.; Jiang M.; Tu Y. F.; Li, M.; Wu, C. *Acc. Chem. Res.* **2001**, *34*, 249.
(22) Zhang, G. Z.; Liu, L.; Zhao, Y.; Ning, F. L.; Jiang, M.; Wu, C. *Macromolecules* **2000**, *33*, 6340.
(23) Tu, Y.; Wan, X.; Zhang, D.; Zhou, Q.; Wu, C. *J. Am. Chem. Soc.* **2000**, *122*, 10201.
(24) Moffitt, M.; Yu, Y.; Nguyen, D.; Graziano, V.; Schneider, D. K.; Eisenberg, A. *Macromolecules* **1998**, *31*, 2190.
(25) Note: It is mentioned in the text that for a nondraining spherical shell with the shell thickness close to zero and a nondraining uniform solid sphere, the ratios of $\langle R_g\rangle/\langle R_h\rangle$ are 1.0 and 0.774, respectively.[19, 22] As to a nondraining uniform spherical shell with a certain thickness T, R_g/R_h is calculated according to ref 23 as:

$$R_g/R_h = \left(\frac{3}{5}\right)\left(\frac{1-((R_h-T)/R_h)^5}{1-((R_h-T)/R_h)^3}\right)^{1/2}$$

R_h is also the outer radius of the spherical shell based on the model. According to this formula, when T/R_h increases from ca. 0 to 1, the value of R_g/R_h decreases from ca. 1 to 0.774 monotonically.

(26) Terreau, O.; Luo, L.; Eisenberg, A. *Langmuir* **2003**, *19*, 5601.
(27) Gohy, J.; Antoun, S.; Jérôme, R. *Macromolecules* **2001**, *34*, 7435.
(28) Gohy, J. F.; Willet, N.; Varshney, S.; Zhang, J. X.; Jérôme, R. *Angew. Chem., Int. Ed.* **2001**, *40*, 3214.

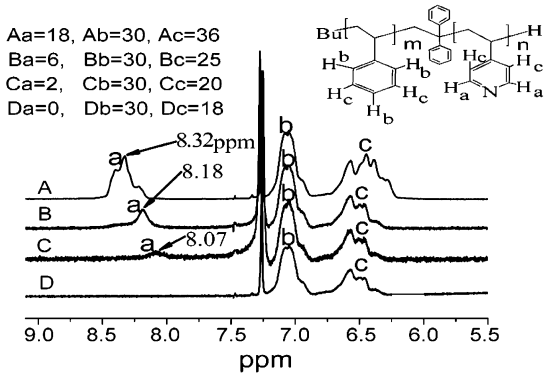

Figure 2. ^{1}H NMR spectra of FA/PS-b-P4VP in $CDCl_3$ at different MR values: MR = 0 (the control experiment, spectrum A); MR = 1/5 (spectrum B); MR = 1/2 (spectrum C); MR = 1/1 (spectrum D). In the inset, K_i refers to the peak area of peak *i* in spectrum K, using dimethyl sulfoxide (DMSO) as an internal standard.

must be very loose. In addition, according to studies reported, the size distribution of block copolymer aggregates seems not to be closely related to the molecular weight distribution of the block copolymer.[26,29,30] In the present study, although the polydispersity index is 1.37, the value of $\mu^2/\langle\Gamma\rangle^2$ of the aggregates at MR of 1/5 is as low as 0.04.

The complexes of *FA*/PS-*b*-P4VP in deuterated chloroform at different *MR* were characterized by ^{1}H NMR. The spectra of the complexes with MR of 0 (the control experiment), 1/5, 1/2, and 1 are shown in Figure 2 as spectra A, B, C, and D, respectively. For clarity, only the spectra from 6.0 to 10.0 ppm were presented. The assignments of the spectra are given as the inset.[31]

In these spectra, the relative intensity of peak b assigned to the hydrogen atoms H_b (inset) in the benzene rings exclusively does not change with the addition of FA and the increase of MR. However, the relative intensities of peak a and peak c, which are associated to H_a in the pyridine rings and H_c in both the pyridine rings and benzene rings, respectively, decrease. When MR equals 1 (spectrum D), peak a disappears completely and the intensity ratio of b to c comes close to 3/2, the number ratio of the H_b to H_c in the benzene rings. In addition, in the ^{1}H NMR spectra, no signals relating to FA are detected.

These ^{1}H NMR data further demonstrate that as the complexation between the block copolymer and FA takes place, the aggregation occurs between the bound pyridine units, so that the mobility of them is restricted, leading to the weakening and even disappearance of P4VP signals[31,32] In addition, it is found by examining the data in Figure 2 that in the cases of MR being 1/5 and 1/2, the decreases in the intensities of peaks a and c compared to pure PS-*b*-P4VP apparently exceed what were expected stoichiometrically. It means that not only the bound pyridine units but also their close neighboring ones lose the mobility and then the corresponding signals diminish. However, those unbound pyridine units relatively far from the bound units remain detectable. Until when MR equals 1, all the pyridine rings are bound with FA molecules and aggregated, leading to the disappearance of their signals. On the other hand, in all the cases, nearly all the

Scheme 1. The Schematic Presentation of the Behaviors of PS-*b*-P4VP/Linear Aliphatic Acids Complexes in Chloroform

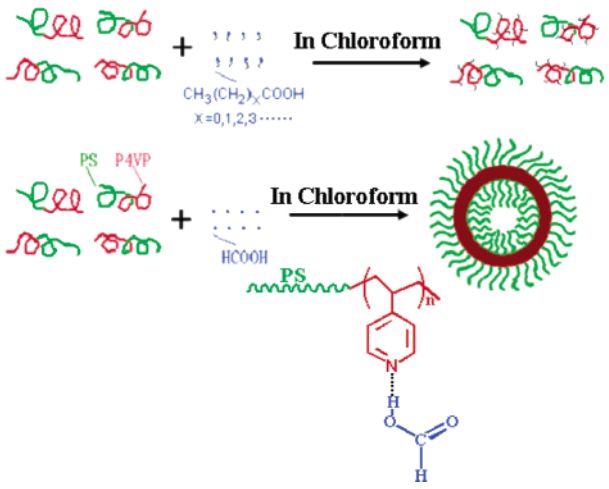

polystyrene chains in the block copolymer are still solvated. These indicate that, in the resultant vesicles, the complexes of FA and P4VP block are aggregated forming the middle solid layer, while the PS blocks form both the inner and outer layers to stabilize the aggregates. It is noted that peak a in spectra B and C shows high field shifts. The more FA that is added, the larger the shift is. As no considerable shift of peak a was found in the ^{1}H NMR spectrum of the stoichiometric complex of acetic acid and PS-*b*-P4VP (in a control experiment made by us), the shifts observed in Figure 2 cannot be attributed to the hydrogen bonding between the carboxyl groups in FA and P4VP units. Therefore, we are inclined to think that those detectable pyridine rings are in fact closely surrounded by aggregated ones, which partially shield the outer magnetic field for those detectable pyridine rings. A similar high-field shift (0.2 ppm) of the methyl group signal due to the shielding was found for the methyl red encapsulated in a dentrimer.[33]

To further demonstrate that it is the insolubility of the "bound units" that drives the aggregation of the complex, we studied the mixture of the vinyl pyridine monomer with FA in chloroform by DLS. The association took place and gave rise to aggregates with $\langle R_h\rangle$ about 100 nm. In addition, mixing homopolymer poly(4-vinylpyridine) with FA resulted in precipitation.

In conclusion, we studied the complexation of PS-*b*-P4VP with a series of linear aliphatic acids in chloroform. The complexes of PS-*b*-P4VP with all the acids except for FA can be molecularly dispersed in the solvent. The lack of the hydrocarbon tails and the higher acidity of FA (as compared with other aliphatic acids) make the complexed units of pyridine/FA insoluble in the low-polar media, driving the self-assembly of the complexes of PS-b-P4VP/FA. The self-assembly results in polymeric vesicles with the P4VP and FA complex as the middle solid layer sandwiched by two solvated PS layers (Scheme 1). This phenomenon has not been reported for the complexes of polymers with low-molecular mass compounds in organic solvents. While it seems that the self-assembly in this case is expectable, the formation of the vesicles with such a regular structure and the high field shift of the signals of some unbound pyridine units are really out of our expectation. Those novel phenomenons, along with the

(29) Sommerdijk, N. A. J. M.; Holder, S. J.; Hirons, R. C.; Jones, R. G.; Nolte, R. J. M. *Macromolecules* **2000**, *33*, 8289.
(30) Cao, L.; Manners, I.; Winnik, M. A. *Macromolecules* **2001**, *34*, 3353.
(31) Chen, D.; Peng, H.; Jiang, M. *Macromolecules* **2003**, 36, 2576.
(32) Liu, S. Y.; Billingham, N. C.; Armes, S. P. *Angew. Chem., Int. Ed.* **2001**, 40, 2328.
(33) Krämer, M.; Stumbè, J. F.; Türk, H.; Krause, S.; Komp, A.; Delineau, L.; Prokhorova, S.; Kautz, H.; Haag, R. *Angew. Chem., Int. Ed.* **2002**, *41*, 4252.

simplicity in the preparation of vesicles, make the system promising in addressing related theoretical and practical problems.

Materials and Methods

PS-*b*-P4VP was prepared and characterized by living anionic polymerization. The weight average molecular weights of the PS and P4VP blocks of the block copolymer are 33 000 and 29 000, respectively, and the M_w/M_n of the block copolymer is 1.37, measured by size exclusion chromatography using DMF as the eluent. All other reagents are of analytical purity and were purified according to standard methods. The solutions of complexes were prepared by adding formic acid dropwise to the solution of the block copolymer under ultrasound.

A modified commercial light scattering spectrometer (ALV/SP-125) equipped with an ALV-5000 multi-τ digital time correlator and an ADLAS DPY425 II solid-state laser (output power = 400 mW at γ = 532 nm) was used. In SLS, the angular dependence of the excess absolute time-averaged scattered intensity of a dilute dispersion, i.e., the Rayleigh ratio $R_{vv}(q)$, can lead to the weight-averaged molar mass M_w, the second virial coefficient A_2, and the *z*-averaged root mean square radius of gyration $\langle R_g^2\rangle_z^{1/2}$, where q is the scattering vector. In this study, the concentration is as low as 10^{-3}g/mL, so the extrapolation to infinite dilution was avoided to prevent any changes in the structure of the aggregates due to dilution. In DLS, the Laplace inversion of a measured intensity−intensity−time correlation function $G^{(2)}(t,q)$ in the self-beating mode can result in a linewidth distribution $G(\Gamma)$. For a pure diffusive relaxation, Γ is related to the translational diffusion coefficient D by $\Gamma/q^2 = D$ or a hydrodynamic radius R_h by $R_h = k_BT/(6\pi\eta D)$ with k_B, T, and η being the Boltzmann constant, absolute temperature, and solvent viscosity, respectively.

The ^{1}H NMR and ^{13}C NMR measurements were performed on Bruker DMX500 (125 and 500 MHz for ^{13}C and ^{1}H, respectively) spectrometer in $CDCl_3$ using TMS as an internal reference. The TEM observations were carried out days after the mixing of FA with the block copolymer. TEM observations were performed with a Philips EM400 microscope at an accelerating voltage of 80 kV. The samples for TEM observation were prepared by depositing a drop of the solution on copper grids, which was coated with thin films of Formvar and carbon successively, and were observed without being stained.

Acknowledgment. The authors thank Professor Chi Wu and Doctor He Cheng of the University of Science and Technology in China for their kind help in completion of this work. This work has been supported by the National Science Foundation of China (50173006 and 50273006).

LA0348721